Journal of Polymer Research (2020) 27: 220
https://doi.org/10.1007/s10965-020-02208-z

ORIGINAL PAPER

Synthesis and characterization of a novel organo-soluble polyimide containing hydroxyl and bis-tert-butyl substituted triphenylpyridine units

Chengyun Yuan[1] · Zhen Sun[2] · Yinghan Wang[1]

Published online: 18 July 2020

Abstract
A new diamine containing hydroxyl and bis-tert-butyl substituted triphenylpyridine units was synthesized and used in the synthesis of polyimides (PIs) via a one-step polymerization. The diamine and PIs were characterized by FTIR and ^{1}H-NMR. The aggregated structure of PIs was amorphous by wide angle X-ray diffraction test and all of them exhibited excellent solubility in most organic solvents. The bis-tert-butyl and triphenylpyridine units endowed PIs excellent thermal stability with 10% weight loss temperatures in the range 493–525 °C and high glass transition temperature in the range 301–344 °C, while the existence of hydroxyl groups provided the possibility for further modification of polymer. The PI membranes had excellent mechanical properties with tensile strength in the range 65–93 MPa. The density of PIs was lower with density in the range 1.266–1.289 g/cm^3. It was foreseeable that PIs will greatly promote the applications of heat-resistant and lightweight PI materials in the future.

Keywords Polyimide · Rigid diamine · Heat resistance · Solubility · Triphenylpyridine

Introduction

Aromatic polyimides (PIs) are receiving more and more attention because of their outstanding comprehensive properties, multi-path synthesis, diverse processing methods and wide application fields [1–5]. The main products included PI membranes [6–9], laminated resin [10], composite materials [11–14], coatings, adhesives [15], fibers [16], separation membranes [17], photosensitive materials [18] and liquid crystal alignment layers [19]. In recent years, the development of high performance PI materials has become a new research hotspot [20]. Due to the rigidity of PI main chain and the strong intermolecular interaction, PIs were kind of polymers material with the excellent heat resistance [21], chemical stability [22] and good mechanical properties [23]. The excellent performance of PI was difficult to achieve by other polymers [24–32]. However, traditional aromatic PI was insoluble and intractable after complete imidization, which made its processing difficult [33, 34]. Therefore, the development of soluble and heat-resistant PI had become the focus of current research. Traditionally, the diamines with flexible or unsymmetrical linkages, ortho-methyl, noncoplanar structures and tert-butyl substituents were designed for the synthesis of PIs aiming at improving solubility by weakening chain-chain interactions and chain packing (crystallinity) [35]. Regrettably, their thermal and mechanical properties were inevitably deteriorated in most cases. Ye et al. reported that a series of PIs containing flexible imide linkages and pendent triphenylamine were synthesized [34]. The PIs exhibited good solubility in polar solvents (MDAc, DMF). But its thermal stability was poor with the temperature of 10% weight loss in range of 395–450 °C. Liu et al. prepared a series of PIs containing quinoxaline units via two-step method and their glass transition temperature and 5% weight loss temperature exceeded 500 °C [36]. Introducing of this unit into the polymer chains will produce intermolecular interaction, which has a great influence on thermal properties of the polymer. D. Simone et al. [37] and Song et al. [2] synthesized a series of PIs containing bulky trifluoromethyl groups. They believed

✉ Yinghan Wang
wang_yh@scu.edu.cn

[1] State Key Laboratory of Polymer Materials Engineering, College of Polymer Science and Engineering, Sichuan University, Chengdu 610065, People's Republic of China

[2] Shanghai KaiYuLin pharmaceutical technology co., LTD, Jiading District, Shanghai 201805, People's Republic of China

that the introduction of bulky trifluoromethyl groups into the polymer chain resulted in great benefits for improving solubility of PIs. But the synthesis of some asymmetric diamines was complicated. In our previous work [38], a series of PIs containing triphenylpyridine units were synthesized. The PIs had excellent thermal stability with 10% weight loss temperatures in excess of 537 °C. However, due to the rigidity of the polymer, its solubility was poor.

In order to balance the heat resistance and solubility of PIs. In this study, a novel bis-tert-butyl substituted triphenylpyridine diamine with hydroxyl group was synthesized. The introduction of bulky tert-butyl groups into the polymer chain could improve the solubility. The triphenylpyridine units could improve the heat resistance of the polymer. The hydroxyl group could improve the solubility of polymer in polar solvents by increasing the polarity of the polymer and provided the possibility for further modification of polymer. Therefore, these PIs were expected to exhibit excellent solubility and heat resistance. To our best knowledge, this diamine had been prepared for the first time. Moreover, the synthesis process was simple and raw materials were cheap. The structure of the PIs was characterized by FTIR, ^{1}H-NMR and elemental analyses. The aggregated structure of PIs was characterized by wide angle X-ray diffraction test. Basic properties, such as solubility, thermal and mechanical properties of PIs were investigated.

Experimental section

Materials

Bromine (Br_2, AR), acetic anhydride (Ac_2O, AR), *m*-Cresol (GC), quinoline (>97%) were bought from Aladin Reagents Co. Ltd. (Shanghai, China). Tert-butyl alcohol (AR), 2,6-di-tert-butyl-p-cresol (AR), sodium thiosulphate ($Na_2S_2O_3$, AR), Pd/C (AR) were obtained from Sinopharm Reagents Co. Ltd. (Shanghai, China). N-methyl pyrrolidone (NMP, AR), hydrazine hydroxide ($N_2H_4.H_2O$), tetrahydrofuran (THF, AR), ammonium acetate (AR), glacial acetic acid (AR), ethanol (AR), methanol (AR) were obtained from Chengdu Kelong Reagents Co. Ltd. (Chengdu, China). 4-Nitroacetophenone (AR) was obtained from Jiangsu Taixing Fine Chemical Co. Ltd. (Jiangsu, China). 4, 4′-Diaminodiphenyl ether (ODA, AR), 4, 4′-diaminodiphenylmethane (MDA, AR), 4, 4′-oxydiphthalicanhydride (ODPA, >99.2%), 3,3′,4,4′-biphenyltetracarboxylic acid dianhydride (BPDA, >98%) and 3,3′,4,4′-benzophenonetetracarboxylic dianhydride (BTDA, >96%) were purchased from Shanghai Research Institute of Synthetic Resins (Shanghai, China). All the solvents and chemicals were used without further purification.

Measurements

^{1}H-NMR was tested by 400 MHz Unity INVOA 400 nuclear magnetic resonance instrument of American Varian company. FTIR was measured by Nicolet 560 FTIR spectrometer of Nicolet company in the United States. Melting point measurement (MP) was made on X4 melting point measurement microscope (Beijing No.3 optical instrument factory) with a heating rate of 10 °C/min. The European EA3000 microanalyzer of Euro vectro S.p.A in USA was used for element analysis. The inherent viscosity of PI solution was measured by Ubbelohde viscometer at 30 ± 0.1 °C. The molecular weight of PI was determined by Gel Permeation Chromatography (GPC), using an Agilent 1100 column, tetrahydrofuran (THF) as eluent and polystyrene standards were used for calibration. The aggregated structure of PIs was characterized by wide angle X-ray diffraction test. Thermogravimetry analysis (TGA) was carried out by DuPont TGA 2100 analyzer at a temperature range of 100 ~ 800 °C and a heating rate of 20 °C/min in a nitrogen atmosphere. The differential scanning calorimetry (DSC) was determined by NETZSCH DSC 204 thermal analyzer at a scan rate of 20 °C/min in flowing nitrogen. The mechanical properties were tested by Instron Universal Tester model 5567 with a load cell of 100 N and a tensile speed of 10 mm/min. The sample size was 4 × 1 cm^2 of membrane the final data was the average of 3–5 samples.

Synthesis of monomer

3,5-Di-tert-butyl-4-hydroxybenzaldehyde (compound 1)

2,6-Di-tert-butyl-p-cresol (2.50 g, 11.3 mmol) and tert-butanol (30 ml) were added to a 250 ml flask and stirred at room temperature. When the solid was dissolved, Br_2 (11.00 g, 68.8 mmol) was added. After the addition, the mixture continued to react at this temperature for 1 h and the temperature was raised to 45 °C. When a large amount of precipitation was generated, the solution was cooled to room temperature, filtered, then the precipitation was washed with 10% sodium thiosulfate aqueous solution and deionized water, respectively. The product was dried in vacuum to obtain 2.26 g (yield 85%) of white solid **1** [39]. Mp: 189–190 °C. FTIR (KBr): 3430, 2955, 1667, 813 cm^{-1}. ^{1}H-NMR (400 MHz, $CDCl_3$), δ = 1.478 (s, 18H, CH_3), 5.838 (s, 1H, OH), 7.727 (s, 2H, Ar-H), 9.851 (s, 2H, CH).

2,4- (3′,5′-Di-tert-butyl-4′-hydroxy) phenyl-2,6-di (4′-nitrophenyl) pyridine (compound 2)

The compound **1** (4.68 g, 20 mmol), 4-nitroacetophenone (6.60 g, 40 mmol), ammonium acetate (30 g) and glacial acetic acid (150 ml) were added to a 500 ml three-neck flask with a

condenser tube. The mixture was refluxed for 8 h, then cooled to room temperature and filtered to obtain a dark brown solid. The crude product was washed with 20% acetic acid solution and deionized water, respectively. The final product was recrystallized from DMF and ethanol to obtain 7.85 g (yield 75%) of light yellow solid [40]. Mp: 270–272 °C. FTIR (KBr): 1518 and 1343 cm^{-1} ($-NO_2$), 1541 and 1593 cm^{-1} (benzene and pyridine ring). ^{1}H-NMR (400 MHz, DMSO-d_6), δ = 1.491 (s, 18H, CH_3), 7.417 (s, 1H, OH), 7.603 (s, 2H, Ar-H), 8.314 (s, 2H, Ar-H), 8.389–8.412 (d, 4H, Ar-H), 8.579–8.619 (d, 4H, Ar-H).

3,4-(3′,5′-Bis-tert-butyl-4′-hydroxy) phenyl-2,6-bis (4″-aminophenyl) pyridine (diamine 3)

The compound **2** (5 g, 10 mmol), Pd/C (0.3 g) and ethanol (50 ml) were added to a 250 ml three-neck flask. The mixture was heated to reflux and hydrazine hydrate (10 ml,) was slowly dripped into reactor under the rapid agitation of a magnetic stirrer. The reactor was kept at this temperature for another 12 h. After the reaction was completed, the ethanol was removed by vacuum distillation. The THF was added to the mixture, filtered to remove Pd/C. The solvent was removed by rotary evaporator. The crude product was recrystallized from DMF and ethanol to obtain 3.6 g (yield 81%) of gray-white solid [41]. Mp: 291–293 °C. FTIR (KBr): 3420 and 3384 cm^{-1} ($-NH_2$). ^{1}H-NMR (400 MHz, DMSO-d_6), δ = 1.470 (s, 18H, CH_3), 5.417 (s, 4H, $-NH_2$), 6.660–6.680 (d, 4H, Ar-H), 7.249 (s, 1H, -OH), 7.467 (s, 2H, Ar-H), 7.626 (s, 2H, Ar-H), 7.955–7.976 (d, 4H, Ar-H).

Synthesis of PIs

The PI1 (ODPA-ODA) was used as a typical example to describe the synthesis route of PIs. In a dry nitrogen atmosphere, diamine **3** (0.300 g, 0.65 mmol), ODPA (0.400 g, 1.30 mmol) and m-cresol (8 ml) were added to a 100 ml three-neck flask. The mixture was stirred for 30 min and ODA (0.129 g 0.65 mmol) was added into reactor. When the mixture formed a homogeneous system, several drops of isoquinoline were dropped into the reactor with a syringe. Then the reaction mixture was stirred for 2 h at room temperature and then heated to 80 °C for 2 h and finally at 180 °C for 24 h. After cooling, the solution was slowly poured into a large amount of methanol under rapid agitation to form a fibrous precipitate. The precipitate was filtered and washed with hot ethanol. PI1 was obtained by drying the filter residue in vacuum at 80 °C for 12 h. FTIR: 3432, 2958, 1779, 1725, 1368 and 744 cm^{-1}. ^{1}H-NMR (400 MHz, DMSO-d_6), δ =1.483 (s, 18H, CH_3), 7.223 (s, 4H), 7. 338 (s, OH), 7.477 (s, 4H), 7.593–7.627 (d, 14H), 8.076–8.125 (d, 6H), 8.448 (s, 4H).

Results and discussion

Monomer synthesis

In this study, the diamine **3** (3,4-(3′,5′-bis-tert-butyl-4′-hydroxy) phenyl-2,6-bis (4″-aminophenyl) pyridine) was successfully synthesized via a three-step synthetic route according to Scheme 1. The FTIR and ^{1}H-NMR spectra of compound 1, compound 2 and diamine 3 were shown in Fig. 1. The FTIR spectrum of compound **1** showed the characteristic band of benzaldehyde was at 1667 cm^{-1}. And the characteristic bands of hydroxyl and alkyl groups were at 3430 and 2955 cm^{-1}, respectively. The ^{1}H-NMR spectrum of compound **1** indicated the characteristic peaks of aldehyde group, phenolic hydroxyl group and benzene ring were at 9.851, 5.838 and 7.727 ppm, respectively. The nitro compound **2** could be prepared by Hantzsch reaction of 4-

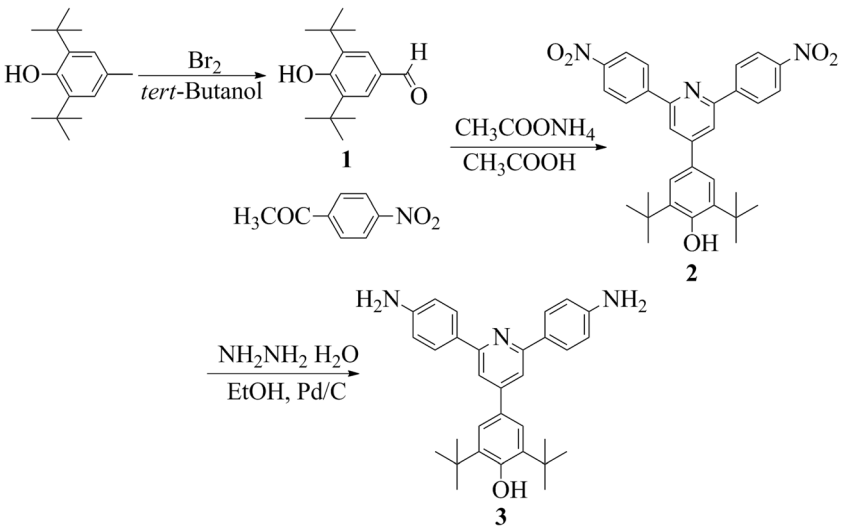

Scheme 1 Synthetic route of the diamine 3

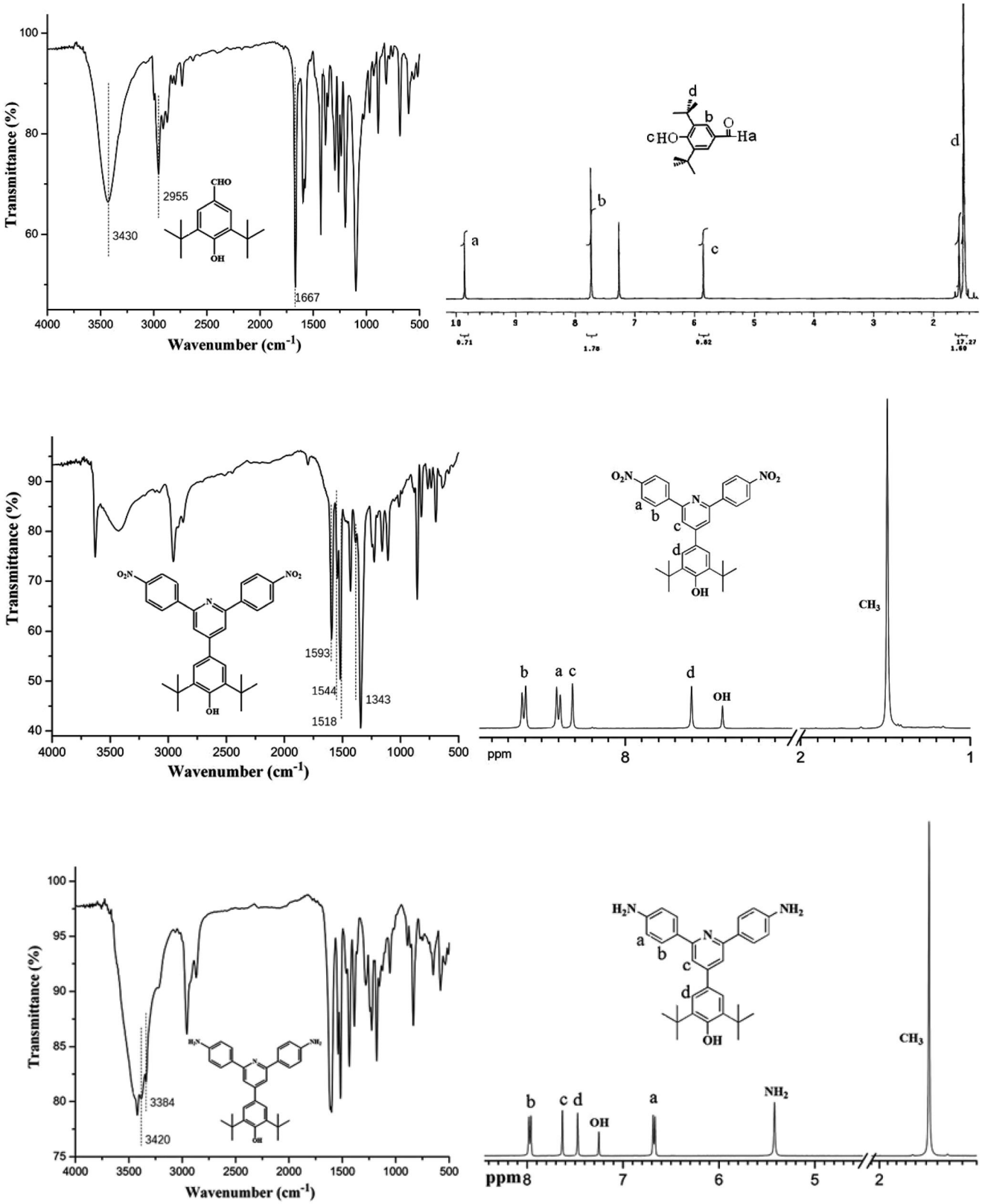

Fig. 1 FTIR and ^{1}H-NMR spectra of compound 1 (in CDCl3), 2 and diamine 3 in DMSO-d_6, respectively

nitroacetophenone and compound **1** in ammonium acetate/acetic acid. The FTIR spectrum of nitro compound **2** showed that the characteristic band of benzaldehyde had disappeared and the characteristic bands of nitro group were at 1518 and

1343 cm^{-1}. And the characteristic bands of pyridine rings and benzene rings were at 1593 and 1544 cm^{-1}, respectively. The new peak at 8.314 ppm in ^{1}H-NMR of compound **2** was also a sign of pyridine ring. The diamine **3** was synthesized by reducing compound **2** in the presence of Pd/C and hydrazine hydrate. The FTIR spectrum of diamine **3** showed that the characteristic bands of the nitro groups had disappeared and the characteristic bands of the amino group were at 3420 and

Scheme 2 Synthesis of PIs

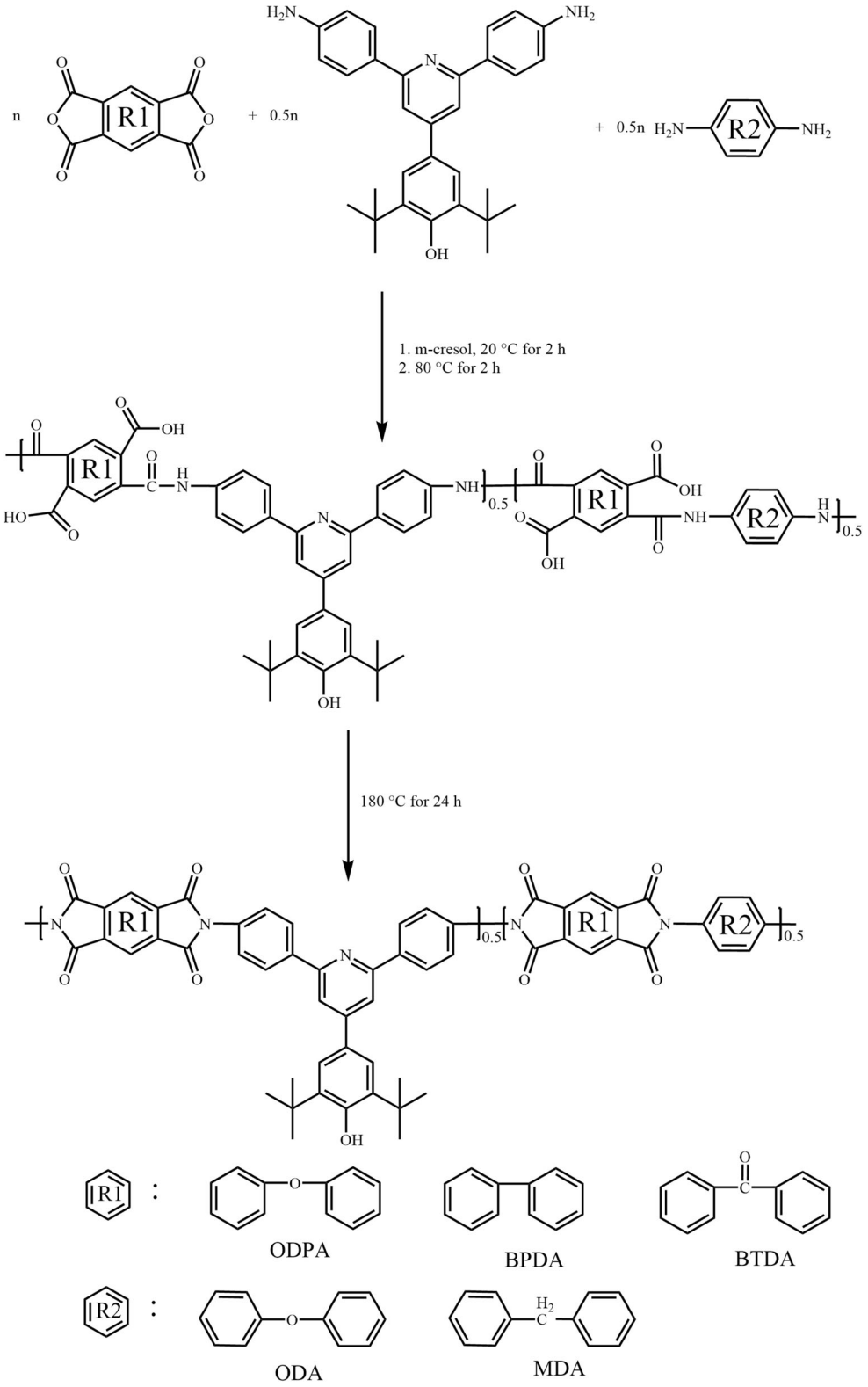

3384 cm^{-1}. The ^{1}H-NMR spectrum of diamine **3** showed that the characteristic peaks of amino group were at 5.417 ppm. The FTIR and ^{1}H-NMR spectra clearly proved that the diamine **3** was synthesized correctly.

Synthesis of polymers

The PIs were synthesized via one-step method in m-cresol (Scheme 2). This reaction used three dianhydrides (ODPA, BTDA and BPDA), two auxiliary diamines (ODA and MDA) and synthesized diamine **3**. The molar ratio of dianhydride: auxiliary diamine: diamine **3** was 100: 50: 50. PI1-PI6 was synthesized according to the formula in Table 1. The FTIR and ^{1}H-NMR spectra of the same series of PIs were roughly same, so the spectrum of PI1 was taken as an example. The FTIR spectrum of PI1 (Fig. 2) showed that the asymmetric and symmetrical stretching vibration bands of C = O on the imide ring were at 1779 and 1725 cm^{-1}, respectively. And the characteristic band of the hydroxyl group was at 3450 cm^{-1}. The ^{1}H-NMR spectrum of PI1 was shown in Fig. 3. It could be seen that the characteristic peaks of the proton of aromatic ring and tert-butyl were at 7.1–8.6 and 1.483 ppm, respectively. From the above characterization and analysis, it could be known that the structure of the synthesized PIs was consistent with the designed polymer. The elemental analysis values and yields of the PIs were listed in Table 1. It could be seen that all PIs had yields above 90% and the loss during processing was small. The test value of hydrogen was slightly higher than the calculated value, which was mainly because the loose PI powder was easy to absorb moisture. In general, the elemental analysis value of PI was basically consistent with the calculated value of the designed structure.

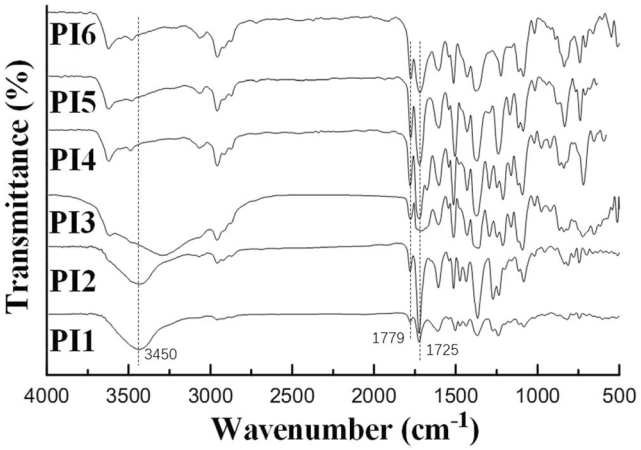

Fig. 2 FTIR spectra of PI1-PI6

Polymer properties

Inherent viscosity and molecular weight

In order to evaluate the polymerization activity of diamine **3**, the inherent viscosity (η_{inh}) and membrane-forming properties of PIs were measured. If PIs had high viscosity and excellent membrane-forming property, it indicated that diamine **3** had good reactivity. The η_{inh} of PIs were between 0.38–0.73 dL/g as shown in Table 2. It could be seen that BTDA-based PIs had the lower η_{inh} than others. This was due to the high reactivity of BTDA resulting in deliquescence during storage. Thus, the molecular weight of BTDA-based PIs was lower than that of others. Because of the solubility of PI1 and PI2 was better than others (as shown in Table 3). In particular, PI1 and PI2 were soluble in THF. So, their molecular weight could be measured. The number average molecular weights of PI1 and PI2 were measured by GPC were 21,000 and 19,000 g/

Table 1 Yields and Elemental Analyses of PIs

PIs	Yield (%)	Elemental analysis (%)			
			C	H	N
PI1 (ODPA: ODA: diamine 3 = 100:50:50)	97	Calcd.	74.19	4.23	5.77
		Found	73.40	5.21	5.16
PI2 (ODPA: MDA: diamine 3 = 100:50:50)	96	Calcd.	75.30	4.41	5.78
		Found	74.52	5.60	5.34
PI3 (BTDA: ODA: diamine 3 = 100:50:50)	95	Calcd.	74.69	4.15	5.66
		Found	73.98	4.79	5.38
PI4 (BTDA: MDA: diamine 3 = 100:50:50)	93	Calcd.	75.78	4.32	5.66
		Found	74.90	5.33	5.51
PI5 (BPDA: ODA: diamine 3 = 100:50:50)	98	Calcd.	76.19	4.35	5.92
		Found	74.98	6.49	6.48
PI6 (BPDA: MDA: diamine 3 = 100:50:50)	96	Calcd.	77.34	4.53	5.93
		Found	76.46	6.78	5.62

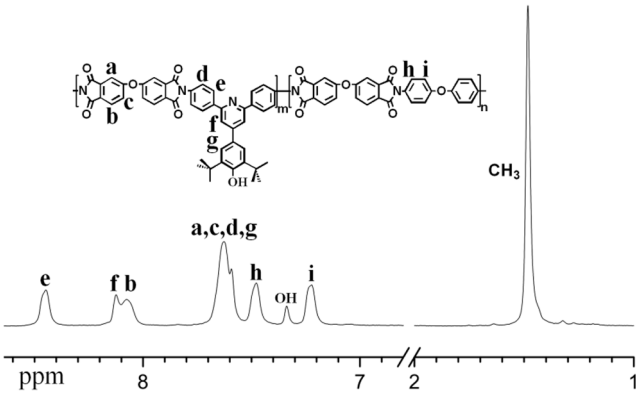

Fig. 3 ^{1}H-NMR spectrum of PI1

mol, respectively. The membrane-forming property of PIs was characterized by the following methods. The NMP solution of PI was poured on a clean glass piece on a heating table, scraped flat with a steel knife and the solvent was slowly evaporated at 120 °C. After the solvent was evaporated, it was placed in an oven and quickly heated to 220 °C for 2 h. The PI membrane was cooled to room temperature and then soaked in distilled water. Finally, the membrane was peeled off, washed with ethanol and dried. With the exception of PI3, all PIs could form dense and ductile membranes, which may be due to the low molecular weight of the BTDA- based polymer. In addition, the membranes based on ODPA and BPDA were lighter in color and PI3 and PI4 were darker in color due to the absorption of light by the structure of BTDA based diphenyl ketone [42].

Solubility property

The WAXD measurements of PIs concluded that the main structure of all the polymers was amorphous as shown in Fig. 4. The WAXD curves of all the PIs were similar. It could be seen that only a very low diffraction intensity and wide diffraction peak was at about 18–24°. And no sharp diffraction peak appeared in the region of small angle. Because the bis-tert-butyl group in diamine **3** increased the spatial volume of the polymer chain segment, damaged the regularity of the chain segment, augmented the free volume and decreased the interaction force between the polymer molecules. At the same time, the two tert-butyl and pyridine ring were in a non-planar state, which also reduced the crystallinity of the polymer. In addition, the tert-butyl group had a large spatial structure which hindered the ordered accumulation of the polymer chain segments [43]. Therefore, all of the PIs were amorphous structures.

The dissolution behavior of PIs was related to the stacking capacity of molecular chains and the intermolecular interactions. The dissolution behavior of PIs in different solvents was listed in Table 3. Because of the presence of bis-tert-butyl, the polymer chain tended to be in the random accumulation state. At the same time, there were a large number of hydroxyl groups in the polymer chain, which made the polymer more polar. Therefore, PIs had better solubility in polar solvents (such as NMP, DMAc and DMF). However, due to the large polarity of PIs, PIs had poor solubility in non-polar solvents ($CHCl_3$ and THF) according to the principle of similar compatibility. Moreover, the pyridine ring on diamine **3** had large polarity and strong affinity with polar solvent molecules [44].

Table 3 Solubility behavior of PIs

PIs	NMP	DMAc	*m*-Cresol	DMF	DMSO	$CHCl_3$	THF
PI1	+++[b]	+++	+++	+++	++	±	+
PI2	+++	+++	++	+++	+++	+	+
PI3	+++	+++	++	+++	+++	±	±
PI4	+++	+++	+++	+++	+++	±	±
PI5	++	+	++	±	±	–	–
PI6	+++	+++	++	±	±	±	–

N-methyl-2-pyrrolidone (NMP), N,N-dimethylformamide (DMF), N,N-dimethylacetamide (DMAc), dimethylsulfoxide (DMSO), trichloromethane ($CHCl_3$), tetrahydrofuran (THF).

[b] +++, 50 mg sample dissolved in 1 mL solvent; ++, 20 mg sample dissolved in 1 mL solvent; +, 10 mg sample dissolved in 1 mL solvent; ±, partially soluble; –, insoluble

Table 2 Inherent viscosity and molecular weight of PIs

PIs	η_{inh}[a](dL/g)	$Mn\times 10^4$	Mw/Mn	Membrane forming ability	Colour
PI1	0.53	2.1	1.7	Uniform and tough	Yellow
PI2	0.49	1.9	2.5	Uniform and tough	Yellow
PI3	0.38	b	b	Uniform and slightly brittle	Brown
PI4	0.41	b	b	Uniform and tough	Brown
PI5	0.73	b	b	Uniform and soft	Slightly yellow
PI6	0.69	b	b	Uniform and soft	Slightly yellow

[a] Inherent viscosity was measured at a concentration of 0.5 g/dL in NMP at 30 °C

[b] The polymer partially soluble or insoluble in THF at room temperature

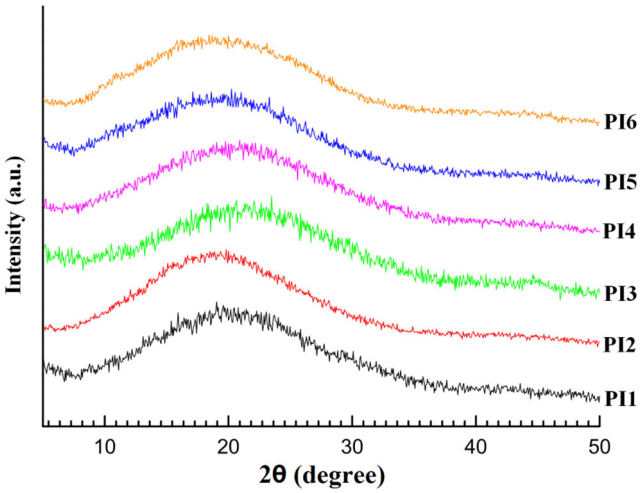

Fig. 4 WAXD diagrams of the PIs

Therefore, the PIs had good solubility in polar solvent. Due to the presence of tert-butyl and pyridine, some PIs were partially soluble in low polar solvents such as $CHCl_3$ and THF. Finally, the structure of dianhydride also had a great influence on the solubility of PIs. PIs based on ODPA and BTDA had better solubility than those based on BPDA. Because the bridge structure of ODPA and BTDA were flexible group, which increased the conformation of the molecular chain and reduced the rotation barrier of the chain segment. Thus, the movement of PI chains was improved and the dispersive ability of polymer chains in solvent was facilitated. In conclusion, the introduction of hydroxyl group and bis-tert-butyl group could significantly improve the solubility of PIs.

Density

With the development of science and technology, high performance and lightweight materials were required in some fields. The density of polymer was closely related to its structure, so the density of the PIs was measured in this study. The test results of PI density were shown in Table 4. Due to the strong interaction between PI molecules, the density of PI was generally between 1.27 and 1.54 g/cm^3, which were relatively high in polymers. The density of PIs in this study was between 1.266 and 1.289 g/cm^3, which were lower than PIs based on PMDA-ODA (1.41 g/cm^3) and ODPA-ODA (1.37 g/cm^3). The main reasons for the low density of PIs were the inclusion of bis-tert-butyl group and random copolymerization. Because the larger steric resistance of the tert-butyl group reduced the intermolecular forces, increased the distance between the molecular chains and prevented the polymer chain segments from being tightly packed. In addition, random copolymerization reduced the density of PIs because it weakened the regularity of molecular chain and loosened the accumulation of polymer [45].

Table 4 Density of PIs

PIs	Density(g/cm^3)
PI1	1.289
PI2	1.278
PI3	1.278
PI4	1.269
PI5	1.267
PI6	1.266

Thermal property

The PIs were a kind of polymers material with excellent comprehensive performance. The thermal performance was one of its excellent properties, which ensured that it could be used for a long time at both high and low temperatures.

The thermal decomposition temperature (T_d) was the main parameter to measure the thermal stability of the polymer. Generally, the thermal stability of polymers was evaluated at temperatures of 5% (T_5) and 10% (T_{10}) weight loss. The TGA curves of PIs were shown in Fig. 5 and the detailed data were listed in Table 5. It was clear that there was basically no mass loss before 350 °C.This indicated that the main chain and imide of PIs synthesized via one step was very complete. In nitrogen atmosphere, T_5 and T_{10} of PIs were 413–438 °C and 493–525 °C, respectively. This proved that this series of PIs had good thermal stability. In addition, the carbon residue rate of PIs at 800 °C was 54.2–58.7%. Because of the presence of a large number of aromatic rings, the carbon residue rate of the polymer was very high, which also indicated that the polymer had good thermal stability. It could be found that the thermal stability of PI based on BTDA was the worst, mainly because the thermal stability of the structure of diphenyl ketone was worse than that of diphenyl ether and biphenyl. To sum up, the PIs we prepared had good thermal stability.

The T_g was one of the characteristic temperatures of polymer materials, which directly affected the service performance

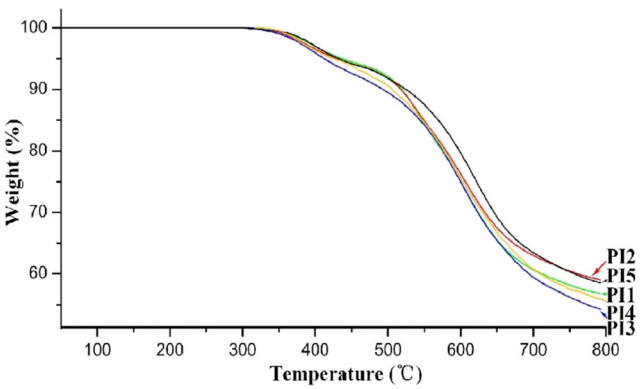

Fig. 5 TGA curves of the PIs

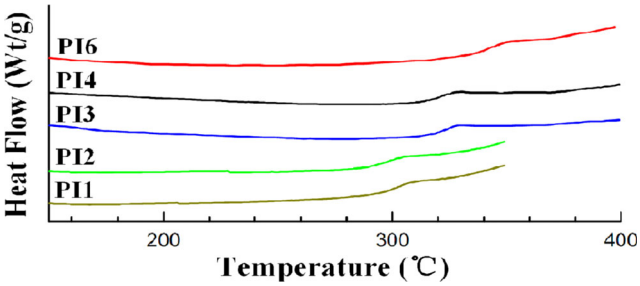

Fig. 6 DSC curves of the PIs

and processing performance of materials. The DSC curves of PIs were shown in Fig. 6 and detailed data were listed in Table 5. It could be seen that all of PIs exhibit high T_g, and the T_g value was between 301 and 344 °C. Because triphenylpyridine and bis-tert-butyl group increased the rotation energy of the polymer chain segment and blocked the movement of the molecular chain. Therefore, the amorphous PIs in this study had high T_g. It was not difficult to see that the T_g of the polymer was closely related to the structure of the dianhydride. Because the diphenyl ether structure of ODPA was the most flexible compared with the structure of diphenyl ketone and biphenyl, the PI1 and PI2 based on ODPA had the lowest T_g. Similarly, since the rigidity of BPDA was the largest compared with other dianhydrides, PIs based on BPDA had the highest T_g. Because of the rigidity of two auxiliary diamines (ODA and MDA) was basically the same size. Therefore, in the case of the same dianhydride, the T_g of PIs based on ODA and MDA were almost the same.

Mechanical property

The mechanical strength of PIs membrane was tested according to the method in the previous literature [46, 47]. The average thickness of the sample was measured by a digital display spiral micrometer instrument. The sample size was 4×1 cm^2 and 3–5 samples were tested for each sample. The experimental data was the average of them. Detailed data on the mechanical properties of PIs were shown in Table 6. The tensile strength, initial modulus and elongation at break of PIs were 65–93 MPa, 1.8–2.3 GPa and 4–15%, respectively. Generally, the molecular weight and viscosity of a polymer were closely related to the mechanical properties of the polymer. Because the molecular weight and viscosity of PI3 were too low, the PI3 film was brittle, so the mechanical properties of PI3 could not be tested. Except for PI3, other PIs had high tensile strength. This was due to the low viscosity of PI3. The higher viscosity made PI5 and PI6 had better mechanical properties.

Table 5 Thermal properties of PIs

PIs	T_g[a] (°C)	T_5[c] (°C)	T_{10}[c] (°C)	R_w[d] (%)
PI1	303	438	520	56.8
PI2	301	430	518	59.0
PI3	322	413	493	54.2
PI4	327	421	508	56.7
PI5	N[b]	433	525	58.5
PI6	344	423	513	58.7

[a] From the second trace of DSC measurements conducted at 20 °C/min heating rate

[b] N: No T_g was obtained

[c] T_5, T_{10} are 5% and 10% weight loss temperature in TGA at 20 °C/min heating rate

[d] R_w, Residual weight retention at 800 °C

Table 6 Mechanical properties of PIs

PIs	Thickness (um)	Tensile strength (MPa)	Elongation break (%)	Tensile modulus (GPa)
PI1	101	74 ± 1	6 ± 0.5	2.0
PI2	103	69 ± 2	4 ± 1	1.9
PI4	98	65 ± 1	4 ± 1.5	1.8
PI5	99	91 ± 2	15 ± 2	2.1
PI6	102	93 ± 1	11 ± 1	2.3

Conclusions

A new bis-tert-butyl substituted triphenylpyridine diamine with hydroxyl group was successfully synthesized and characterized. Moreover, the new diamine was used for the first time polymerization to produce a series of highly soluble and heat-resistant PIs. The bis-tert-butyl group increased the molecular spacing, reduced the intermolecular forces, prevented the molecular chain from being tightly packed and weakened the crystallization capacity of the polymer. In addition, the triphenylpyridine unit increased the rigidity of the main chain and thus effectively reduced the kinematic capacity of the chain segment. Therefore, PIs were completely amorphous and they exhibited excellent solubility and high T_g (301–344 °C) values. The PIs had good thermal stability with the T_{10} in the range 493–525 °C and lower density in the range 1.266–1.289 g/cm^3. Finally, the existence of hydroxyl group provided a realistic possibility for further functionalization of PIs. It was foreseeable that PIs will greatly promote the applications of heat-resistant and lightweight PI materials in the future.

Acknowledgements This work was supported by the National Natural Science Foundation of China (Grant No. 51173115).

References

1. Cherkashina NI, Pavlenko VI, Noskov AV (2019) Synthesis and property evaluations of highly filled polyimide composites under thermal cycling conditions from −190 °C to +200 °C. Cryogenics 104:102995
2. Song G, Chen C, Wang X, Yao J (2019) Synthesis and properties of polyimides derived from 2,2'-dichloro-4,4',5,5'-biphenyltetracarboxylic dianhydride. Polymer 183:121862
3. Park C-Y, Kim E-H, Kim JH, Lee YM, Kim J-H (2018) Novel semi-alicyclic polyimide membranes: synthesis, characterization, and gas separation properties. Polymer 151:325–333
4. Yang Y, Lu H, Liu J, Shen Y (2018) Synthesis and binary/ternary write-once read-many-times electrical memory behaviors of carbazole-based polyimides bearing flexible linkage segment. Eur Polym J 108:10–19
5. Yang Y, Xia J, Ding Z, Zheng Y, Ding S, Shen Y (2018) Synthesis and resistive switching characteristics of polyimides derived from 2,7-aryl substituents tetraphenyl fluorene diamines. Eur Polym J 108:85–97
6. Lanč M, Sysel P, Šoltys M, Štěpánek F, Fónod K, Klepić M, Vopička O, Lhotka M, Ulbrich P, Friess K (2018) Synthesis, preparation and characterization of novel hyperbranched 6FDA-TTM based polyimide membranes for effective CO2 separation: effect of embedded mesoporous silica particles and siloxane linkages. Polymer 144:33–42
7. Xu J, Ni H, Wang S, Wang Z, Zhang H (2015) Direct polymerization of a novel sulfonated poly(arylene ether ketone sulfone)/sulfonated poly(vinylalcohol) crosslinked membrane for direct methanol fuel cell applications. J Membr Sci 492:505–517
8. Zhang Y, Liu J, Wu X, Bi H, Jiang G, X-x Z, Qi L, Zhang X (2018) Synthesis and characterization of thianthrene-containing preimidized soluble polyimide resins and the derived films with high refractive indices and good optical transparency. J Polym Res 26:2
9. Zhang Y, Tan Y-y, J-g L, X-x Z, M-g H, Jiang G-l WX, Zhang X (2019) Molecular design, synthesis and characterization of intrinsically black polyimide films with high thermal stability and good electrical properties. J Polym Res 26:171
10. Tseng IH, Hsieh T-T, Lin C-H, Tsai M-H, Ma D-L, Ko C-J (2018) Phosphinated polyimide hybrid films with reduced melt-flow and enhanced adhesion for flexible copper clad laminates. Prog Org Coat 124:92–98
11. Kurinchyselvan S, Hariharan A, Prabunathan P, Gomathipriya P, Alagar M (2019) Fluorinated polyimide nanocomposites for low K dielectric applications. J Polym Res 26:207
12. Rafiee Z, Golriz L (2015) Polyimide nanocomposite films containing α-Fe2O3 nanoparticles. J Polym Res 22:630
13. Zhang Y, Liu J, Wu X, Guo C, Qu L, Zhang X (2018) Trisilanolphenyl-POSS nano-hybrid poly(biphenyl dianhydride-p-phenylenediamine) polyimide composite films: miscibility and structure-property relationship. J Polym Res 25:139
14. Akhter T, Saeed S, Siddiqi HM, Park OO, Ali G (2014) Synthesis and characterization of novel coatable polyimide-silica nanocomposites. J Polym Res 21:332
15. Wang K, Yuan X, Zhan M (2017) Comparison between microwave and thermal curing of a polyimide adhesive end-caped with phenylethynyl groups. Int J Adhes Adhes 74:28–34
16. Xiao M, Zhang X, Xiao W, Du J, Song H, Ma Z (2019) The influence of chemical constitution on the structure and properties of polyimide fibre and their graphite fibre. Polymer 165:142–151
17. Mansourpanah Y, Ostadchinigar A (2017) Preparation of chemically attached polyamide thin film membrane using different diamines: separation and computational investigation. J Polym Res 24:26
18. Chen M-H, Lai C-C, Chen H-L, Lin Y-H, Huang K-Y, Lin C-H, Hsiao H-T, Liu L-C, Chen C-M (2018) Preparation of photosensitive polyimides (PSPIs) and their feasible evaluation for lithographic insulation patterns (LIPs) of integrated circuits (ICs) without negative photoresists. Mater Sci Semicond Process 88:132–138
19. Gong S, Liu M, Xia S, Wang Y (2014) Synthesis of novel soluble polyimides containing triphenylamine groups for liquid crystal vertical alignment layers. J Polym Res 21:542
20. Wu Q, Ma X, Zheng F, Lu X, Lu Q (2019) High performance transparent polyimides by controlling steric hindrance of methyl side groups. Eur Polym J 120:109235
21. Ou X, Lu X, Chen S, Lu Q (2020) Thermal conductive hybrid polyimide with ultrahigh heat resistance, excellent mechanical properties and low coefficient of thermal expansion. Eur Polym J 122:109368
22. Simón-Herrero C, Chen X-Y, Ortiz ML, Romero A, Valverde JL, Sánchez-Silva L (2019) Linear and crosslinked polyimide aerogels: synthesis and characterization. J MATER RES TECHNOL 8(3): 2638–2648
23. Zhao H, Yang C, Li N, Yin J, Feng Y, Liu Y, Li J, Li Y, Yue D, Zhu C, Liu X (2019) Electrical and mechanical properties of polyimide composite films reinforced by ultralong titanate nanotubes. Surf Coat Technol 360:13–19
24. Reddy KR, Hassan M, Gomes VG (2015) Hybrid nanostructures based on titanium dioxide for enhanced photocatalysis. Appl Catal A-Gen 489:1–16
25. Reddy KR, Sin BC, Yoo CH, Sohn D, Lee Y (2009) Coating of multiwalled carbon nanotubes with polymer nanospheres through microemulsion polymerization. J Colloid Interface Sci 340(2):160–165
26. Hassan M, Reddy KR, Haque E, Minett AI, Gomes VG (2013) High-yield aqueous phase exfoliation of graphene for facile nanocomposite synthesis via emulsion polymerization. J Colloid Interface Sci 410:43–51
27. Reddy KR, Lee K-P, Gopalan AI, Kang H-D (2007) Organosilane modified magnetite nanoparticles/poly(aniline-co-o/m-aminobenzenesulfonic acid) composites: synthesis and characterization. React Funct Polym 67(10):943–954
28. Zhang Y-P, Lee S-H, Reddy KR, Gopalan AI, Lee K-P (2007) Synthesis and characterization of core-shell SiO2 nanoparticles/poly(3-aminophenylboronic acid) composites. J Appl Polym Sci 104(4):2743–2750
29. Zhang J, Lu Z, Wu M, Wu Q, Yang J (2015) Facile fabrication of poly(acrylic acid) hollow nanogels via in situ Pickering miniemulsion polymerization. Polym Chem 6:6125–6128
30. Choi SH, Kim DH, Raghu AV, Reddy KR, Lee H-I, Yoon KS, Jeong HM, Kim BK (2011) Properties of Graphene/waterborne polyurethane Nanocomposites cast from colloidal dispersion mixtures. J Macromol Sci Part B-Phys 51(1):197–207
31. Khan MU, Reddy KR, Snguanwongchai T, Haque E, Gomes VG (2016) Polymer brush synthesis on surface modified carbon nanotubes via in situ emulsion polymerization. Colloid Polym Sci 294: 1599–1610
32. Reddy KR, Lee KP, Gopalan AI (2007) Self-assembly directed synthesis of poly(ortho-toluidine)-metal(gold and palladium) composite nanospheres. J Nanosci Nanotechnol 7:3117–3125
33. Li Q, Liu S, Xu M, Pan X, Li N, Zhu J, Zhu X (2020) Selenide-containing soluble polyimides: high refractive index and redox responsiveness. Eur Polym J 122:109358
34. Ye Q, Zhang B, Yang Y, Hu X, Shen Y (2020) Binary/ternary memory behavior of organo-solubility polyimides containing flexible imide linkages and pendent triphenylamine or 3, 4, 5-trifluobenzene moieties. Eur Polym J 125:109473
35. Yi L, Huang W, Yan D (2017) Polyimides with side groups: synthesis and effects of side groups on their properties. J Polym Sci A Polym Chem 55(4):533–559

36. Liu T-Q, Zheng F, Ding T-M, Zhang S-Y, Lu Q (2019) Design and synthesis of a novel quinoxaline diamine and its polyimides with high-Tg and red color. Polymer 179:121612
37. Simone CD, Vaccaro E, Scola DA (2019) The synthesis and characterization of highly fluorinated aromatic polyimides. J Fluor Chem 224:100–112
38. Gu Y, Sun Z, Gong S, Zhang H, Gong Q, Liu L, Wang Y (2015) Synthesis and characterization of soluble and thermally stable triphenylpyridine-containing aromatic polyimides. J Mater Sci 50: 6552–6558
39. Shadyro OI, Sorokin VL, Ksendzova GA, Savinova OV, Samovich SN, Pavlova NI, Polozov GI, Boreko EI (2016) Synthesis and antiviral activity of Hydroxy-substituted Benzaldehydes and related compounds. Pharm Chem J 50(3):156–158
40. Wang H, Zhao W, Du J, Wei F, Chen Q, Wang X (2019) An efficient one pot three-component synthesis of 2,4,6-triarylpyridines using triflimide as a metal-free catalyst under solvent-free conditions. RSC Adv 9:5158–5163
41. Ling F, Shen L, Pan Z, Fang L, Song D, Xie Z, Zhong W (2018) B(C6F5)3-catalyzed oxidative deamination/cyclization cascade reaction of benzylamines and ketones for the synthesis of 2,4,6-triarylpyridines. Tetrahedron Lett 59:3678–3682
42. Hu X, Mu H, Wang Y, Wang Z, Yan J (2018) Colorless polyimides derived from isomeric dicyclohexyl-tetracarboxylic dianhydrides for optoelectronic applications. Polymer 134:8–19
43. Liu J-J, Tan J-H, Zeng Y, Liu Y-W, Zeng K-J, Liu Y-J, Wu R-M, Chen H (2017) Synthesis and characterization of high-barrier polyimide containing rigid planar moieties and amide groups. Polym Test 61:83–92
44. Wang S, Ma S, He H, Ai W, Wang D, Zhao X, Chen C (2019) Aromatic polyimides containing pyridine and spirocyclic units: preparation, thermal and gas separation properties. Polymer 168: 199–208
45. Liu Y, Guo J, Wang J, Zhu X, Qi D, Li W, Shen K (2020) A novel family of optically transparent fluorinated hyperbranched polyimides with long linear backbones and bulky substituents. Eur Polym J 125:109526
46. Hana SJ, Leea H-I, Jeonga HM, Kimb BK, Raghuc AV, Reddy KR (2014) Graphene modified Lipophilically by stearic acid and its composite with low density polyethylene. J Macromol Sci Part B-Phys 53:1193–1204
47. Son DR, Raghu AV, Reddy KR, Jeong HM (2016) Compatibility of thermally reduced Graphene with polyesters. J Macromol Sci Part B-Phys 55(11):1099–1110